Engineering with Computers (2020) 36:1849–1856
https://doi.org/10.1007/s00366-019-00800-6

ORIGINAL ARTICLE

Micro-seismic source location determined by a modified objective function

L. Z. Wu[1] · S. H. Li[1] · R. Q. Huang[1] · S. Y. Wang[2]

Received: 31 July 2018 / Accepted: 10 June 2019 / Published online: 29 June 2019

Abstract
The exact localization of micro-seismic sources is of significant importance in micro-seismic monitoring technology. The methods determining arrival time and time difference of micro-seismic source locations in engineering are introduced. The factors affecting the accuracy of the micro-seismic source location are analysed. To improve the accuracy of micro-seismic source localization, an objective function is used to examine the source, and a new method for locating micro-seismic sources is proposed. To make full use of the monitoring data of each geophone, the L2-norm and variance function are combined to improve the overall accuracy of the positioning and the stationarity of the objective function of each geophone equation. Finally, a particle swarm optimization is employed to search for the source location. The effectiveness of the improved method is verified by two case studies, and the results indicate that the proposed method is better than conventional approaches. The proposed method is simple and easy to perform.

Keywords Micro-seismic source localization · Objective function · Particle swarm optimization · Mathematical model

1 Introduction

When the energy within a rock mass reaches a certain threshold value, microcracks occur. This process is accompanied by the release of elastic waves. The release of elastic waves is called micro-seismicity [24, 31]. Since the 1930s, the location of such micro-seismicity has been a problem, and the search for micro-seismic phenomena has gained increasing attention. Microseismic monitoring has been successfully applied in practical engineering, such as South Africa's Integrated Seismic System, Canada's Engineering Seismology Group, and Poland's Seismological Observation System [8, 13, 14, 26]. This technique plays an important role in the early warning and prediction of geological hazards including landslide [15, 16, 27, 28, 32]. This technology has been widely used in fields such as mining, underground, and tunnel engineering [4, 7, 22, 23]. Compared with traditional deformation monitoring, micro-seismic monitoring technology shows remarkable three-dimensional space and real-time advantages and is not limited to point measurements. However, source location is a fundamental problem for micro-seismic monitoring. Hence, effective source localization algorithms are vital in developing micro-seismic monitoring technology [9, 19].

Source localization is a hot research topic that involves geophysics, geotechnical engineering, and information science. Early localization algorithms included the Geiger method [11], joint inversion method [6], and relative positioning method [25]. Recently, some new methods to locate seismic sources have been developed from engineering applications [5, 9, 17, 19, 21]. Based on the mathematical transformation of the arrival time, Dong and Li [5] proposed a source localization method that does not incorporate the wave velocity. Li et al. [17] improved the method of Dong and Li [5] to provide a simple iterative source search model without considering the velocity. Feng et al. [9] proposed a piecewise velocity model and determined the seismic source position using a particle swarm algorithm. Li et al. [19, 20] used the simplex algorithm to capture the micro-seismic source location, with an L1 norm objective function improving the accuracy of source location.

✉ R. Q. Huang
hrq@cdut.edu.cn

[1] State Key Laboratory of Geohazard Prevention and Geoenvironment Protection, Chengdu University of Technology, Chengdu 610059, Sichuan, People's Republic of China

[2] Department of Civil, Surveying and Environmental Engineering, ARC Centre of Excellence for Geotechnical Science and Engineering, The University of Newcastle, Callaghan, NSW 2308, Australia

In practice, the accuracy of locating the micro-seismic source is affected by many factors, such as signal observation, the velocity model, the objective function, and the layout of the geophone. These factors are interrelated, and inaccuracies in any one of them may lead to an increase in the source location error. Therefore, the influence of various factors should be minimized to improve the accuracy of source localization.

In engineering, a uniform velocity model is usually used for convenience [12]. Some researchers have gradually established a multi-directional velocity model [4]; however, this requires a large quantity of wave velocity measurement data, which is difficult for complex rock formations. The positioning method is improved from the objective function, and the mathematical processing is convenient [18].

According to the objective function of the factors influencing micro-seismic source localization, the characteristics of the wave velocity and the effect of the objective function on positioning accuracy are analysed. Based on an improved objective function, a new method of micro-seismic source location is developed.

2 General model of micro-seismic source location

2.1 Mathematical model of micro-seismic source location

In practical engineering, micro-seismic monitoring obtains useful information by analysing signals from rock fractures, which can provide a scientific basis for evaluating rock mass stability [29, 30]. A number of geophones are arranged in a monitoring area around the seismic source. If micro-seismic events occur in the region, the signal is captured by the signal geophone and converted into a voltage or charge. Multi-point synchronous data acquisition from each geophone observation enables the position and velocity to be determined in the location equation. As a result, the space–time parameters of the micro-seismic source can be obtained, and the source localization can be realized. In practical applications, the P-wave is typically used for localization because of difficulties in measuring the S-wave. In Fig. 1, point O is the source, and A–J are the geophones. The P-wave signal generated by the source propagates in all directions, and the actual P-wave velocity is not isotropic. However, for convenience of the mathematical description, the P-wave velocity is usually assumed to be the same in all directions [5, 17, 19, 20].

The ideal mathematical model of micro-seismic positioning is written as follows:

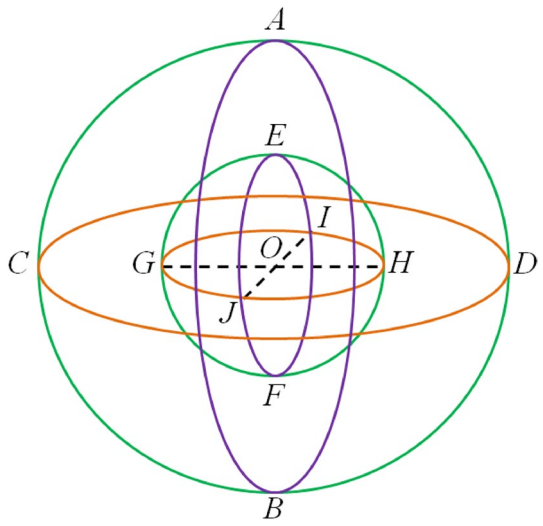

Fig. 1 Sketch of the micro-seismic source location

$$\sqrt{(x_i - x_o)^2 + (y_i - y_o)^2 + (z_i - z_o)^2} = v_p(t_i - t_0), \tag{1}$$

where (x_i, y_i, z_i) are the coordinates of geophone i ($i = 1, 2, \ldots, n$), v_p is the P-wave velocity, t_i is the observed time of the geophone i, t_0 is the shock time, and (x_o, y_o, z_o) are the source coordinates. The parameters (x_o, y_o, z_o), v_p, and t_0 are unknown.

2.2 Method of determining the micro-seismic source

Optimization techniques such as genetic algorithms (GA) and particle swarm optimization (PSO) have been used to solve Eq. (1). When an optimization algorithm is employed, the objective function can be specified. By transforming Eq. (1), the trigger times (TT) and time difference (TD) methods, which are widely used for actual micro-seismic source location, are developed.

The TT method is described as follows [5, 17]:

$$\min \text{fun} = \sum_{i=1}^{n} \left(t_i - \frac{\sqrt{(x_i - x_o')^2 + (y_i - y_o')^2 + (z_i - z_o')^2}}{v_p'} - t_0' \right)^2, \tag{2}$$

where the source location (x_o', y_o', z_o'), P-wave velocity v_p' obtained from inversion and seismic time t_0' are unknown.

The TD method is written as [5, 17, 19] follows:

$$\min \text{fun} = \sum_{i=1}^{n-1} \left(t_{i+1} - t_i - \frac{\left(\sqrt{(x_{i+1} - x_o')^2 + (y_{i+1} - y_o')^2 + (z_{i+1} - z_o')^2} - \sqrt{(x_i - x_o')^2 + (y_i - y_o')^2 + (z_i - z_o')^2} \right)}{v_p'} \right)^2, \tag{3}$$

where the source location (x_o', y_o', z_o') and P-wave velocity (v_p') are unknown.

Equation (2) or (3) is solved by an optimization method, and the minimum value of the objective function is taken as the inverse solution of the seismic source.

3 Error analysis of source localization

Micro-seismic localization contains many types of errors related to the spatial coordinates of the geophone, anisotropy of the wave velocity, and observed time. Errors are produced by known parameters in the micro-seismic location, and it is difficult to obtain an accurate solution. Therefore, it is very important to select an approximate solution that satisfies the engineering requirements. Spatial coordinate errors and arrival time errors can be corrected by improving instrument observations. This section is mainly concerned with the effects of velocity errors and the objective function on the source localization.

Micro-seismic source location techniques have been widely applied in engineering because methods based on a uniform velocity are easy to implement. However, the actual wave velocity is not uniform. The error caused by the uniform velocity model has gained increasing attention. To illustrate the non-uniformity of the wave velocity, the velocity is calculated using data (see Table 1) from a previous project [10]; the positional arrangement of the geophones is shown in Fig. 2, and the calculated results are shown in Fig. 3. Figure 3a describes the velocity of the seismic source to each geophone calculated by the TT method. The velocity in Fig. 3b was calculated using the TD method, that is, by comparing the velocity at each pair of geophones. As there are 11 geophones, there are $C_{11}^2 = 55$ sets of velocities. In Fig. 3, the velocity difference at each geophone is

Table 1 The monitoring data [10]

Geophone	*X* (m)	*Y* (m)	*Z* (m)	Observed time (ms)
A	67,354.79	52037.4	538.7161	34.66
B	67,315.86	52,011.14	533.1324	28.34
C	67,276.13	51,998.22	548.0021	25.03
D	67,342.23	52,070.47	498.8039	30.28
E	67,296.19	52,044.93	497.5552	20.99
F	67,213.53	52,037.89	484.8445	8.01
G	67,147.72	52,030.86	498.9762	16.97
H	67,095.10	52,007.59	480.9712	26.79
I	67,052.20	52,003.89	498.5405	35.70
J	67,236.59	52,121.75	430.1000	24.35
K	67,178.87	52,112.05	430.5220	22.64

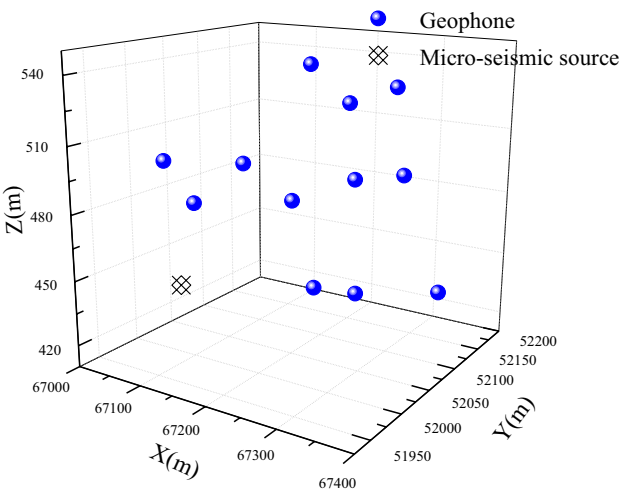

Fig. 2 Positional arrangement of the geophones

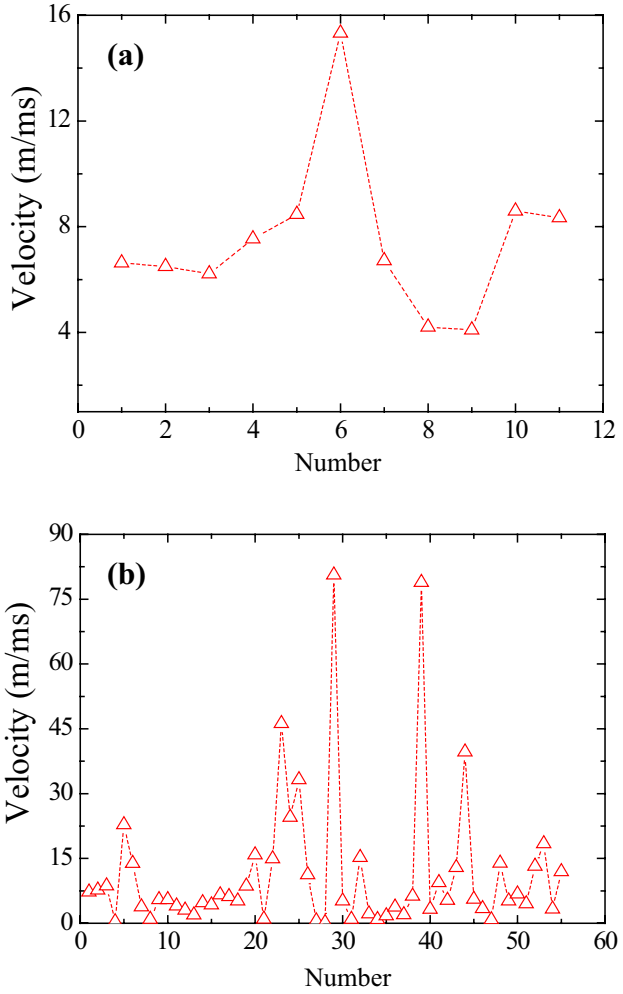

Fig. 3 Velocity calculations: **a** TT method and **b** TD method

remarkable. According to the principle of the arrival time difference, the velocity calculated by each pair of geophones is different.

The objective function of micro-seismic source location has an important influence on the positioning result. An objective function combining P-wave and S-wave arrival times has been proposed [18]. However, its equilibrium coefficient needs to be determined empirically. The current method is to minimize the objective function to obtain the positioning results. The known parameters of micro-seismic location produce errors; thus, the localization results from minimizing the objective function are inconsistent with the actual conditions. Figure 4 compares the objective function [f, see Eqs. (2) and (3)] and the positioning accuracy (d), which is the Euclidean distance between the estimated and actual locations in the search region (confined by boundary conditions for algorithm settings). Actual source positions of ± 10 m, ± 100 m, and ± 1000 m correspond to small, medium, and large scales, respectively.

In Fig. 4, for each scale, the objective function of the micro-seismic location problem has many extreme points. Therefore, the source search is a complex multi-extremum optimization problem. At different scales, the source coordinates of the global minimum of the objective function are not equal to those of the minimum distance function. The error of the micro-seismic positioning system is difficult to eliminate. Enlarging the search area increases number of minimum points of the objective function; thus, searching becomes more difficult. It is necessary to determine the boundary conditions according to the actual conditions to reduce difficulties in searching the micro-seismic location.

In summary, the velocity model and the objective function have a significant effect on micro-seismic source location. In the next section, a micro-seismic source localization algorithm is proposed to improve the accuracy of micro-seismic source location.

4 Improvement of the micro-seismic source location method

4.1 Modification of the objective function

As it is difficult to locate the micro-seismic source accurately with a single source location, a combined objective function for micro-seismic source localization was introduced by Li et al. [18]. However, the method of combining P-wave and S-wave arrival times increases the technical difficulty.

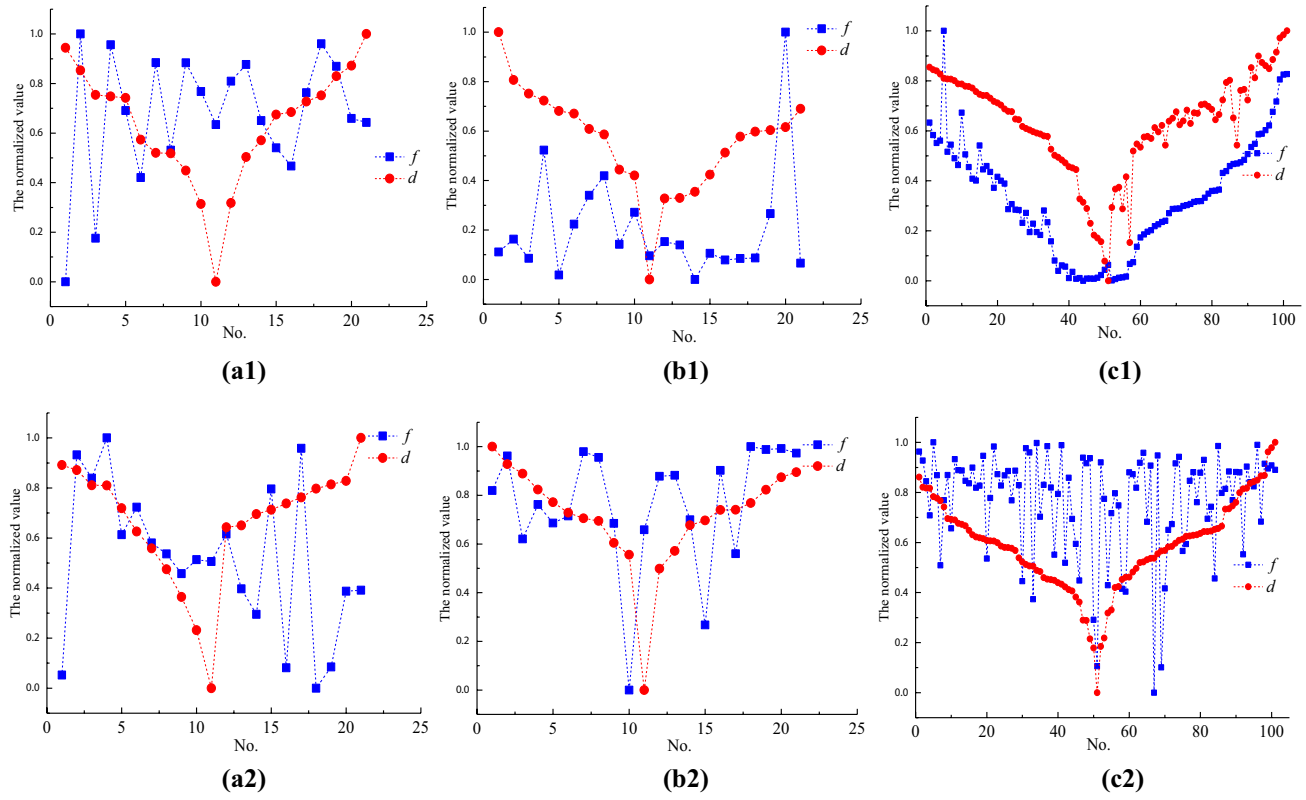

Fig. 4 Comparison of the objective function value and location accuracy: **a1** small scale (TT), **a2** small scale (TD), **b1** medium scale (TT), **b2** medium scale (TD), **c1** large scale (TT), and **c2** large scale (TD)

Although the velocity model and the objective function are the factors affecting the location error of the micro-seismic source, it is difficult to modify the velocity model, while the correction of the objective function becomes much easier. Therefore, the following objective function is proposed:

$$\min \text{fun} = \alpha \sum_{i=1}^{n} \left(t_i - \frac{\sqrt{(x_i - x_o')^2 + (y_i - y_o')^2 + (z_i - z_o')^2}}{v_p'} - t_0' \right)^2 + \beta D \left(\left(t_i - \frac{\sqrt{(x_i - x_o')^2 + (y_i - y_o')^2 + (z_i - z_o')^2}}{v_p'} - t_0' \right)_{i=1,\ldots,n} \right) \tag{4}$$

where D is the variance function ($D(w_i)_{i=1,2,\ldots,n} = \sum_{i=1}^{n} \left(w_i - \left(\sum_{i=1}^{n} w_i \right) / n \right) / n,$), which can be calculated according to probability theory; and α, and β are the weight coefficients ($0 \le \alpha, \beta \le 1$, generally, $\alpha = \beta$). The first term in Eq. (4) can be considered the L2-norm (compared with the L1-norm, the L2-norm is more holistic, while the L1-norm is sparse), which is used to evaluate the accuracy of the positioning results. The second term is used to characterize the stability of the overall results. The variance function is used to evaluate the positioning accuracy of each geophone. The smaller the variance is, the more stable the data becomes, which can be used to characterize the information utilization ratio of each detector. Based on the TD method, another improved objective function can also be given by

$$\min \text{fun} = \alpha \sum_{i=1}^{n-1} \left(t_{i+1} - t_i - \frac{\left(\sqrt{(x_{i+1} - x_o')^2 + (y_{i+1} - y_o')^2 + (z_{i+1} - z_o')^2} - \sqrt{(x_i - x_o')^2 + (y_i - y_o')^2 + (z_i - z_o')^2} \right)}{v_p'} \right)^2 + \beta D \left(\left(t_{i+1} - t_i - \frac{\left(\sqrt{(x_{i+1} - x_o')^2 + (y_{i+1} - y_o')^2 + (z_{i+1} - z_o')^2} - \sqrt{(x_i - x_o')^2 + (y_i - y_o')^2 + (z_i - z_o')^2} \right)}{v_p'} \right)_{i=1,2,\ldots,n-1} \right) \tag{5}$$

4.2 Particle swarm optimization

PSO [1] is one of the most representative intelligent optimization algorithms. Unlike traditional optimization methods, PSO does not need a derivative function and is easy to implement with fast convergence. The complexity of the PSO algorithm is obviously lower than that of other intelligent optimization algorithms [2], such as the GA, artificial fish swarm algorithm, and artificial bee colony algorithm. The advantages of PSO have been seen in many engineering fields. In this algorithm, the solution of the problem is represented by the particle position x.

To realize local and global optimization, the current velocity $\boldsymbol{v}$ and particle position x are iterated until they satisfy some preset conditions. The key equation of the PSO algorithm is expressed as follows:

$$v_i^{k+1} = w v_i^k + c_1 r_1 (p_i^k - x_i^k) + c_2 r_2 (g_i^k - x_i^k), \tag{6}$$

$$x_i^{k+1} = x_i^k + v_i^{k+1}, \tag{7}$$

where v_i^k, and x_i^k are the particle velocity and position after k iterations, respectively; p_i^k is the local optimal position of the particles; g_i^k is the global best position of the particles, and c_1, and c_2 are the learning factor and the step adjustment parameter, respectively. The inertia weight w is an important parameter in the PSO algorithm that balances the effectiveness of global and local searches. The value of w generally decreases with each iteration according to

$$w_i = w_{\max} - \frac{i}{N}(w_{\max} - w_{\min}), \tag{8}$$

where $w_{\max}=0.9$, $w_{\min}=0.4$ and i/N is the ratio of the iteration number to the total (maximum) number of iterations. By linearly decreasing the inertia coefficient, the global search performed at the initial stage of the algorithm gradually becomes a local search in the later stages of the algorithm.

In this paper, the PSO algorithm is employed to search the source location. If Eq. (4) is the objective function, then the number of the optimization variable is 5. If Eq. (5) is the objective function, then the number of the optimization variable is 4. The flow chart of the improved method is given in Fig. 5. In addition to the PSO algorithm, the other optimization algorithms can also be employed. The PSO algorithm is mainly considered in this paper because it is easy to perform. Among the optimization algorithms, genetic algorithm and particle swarm optimization are the two most common algorithms. Compared with genetic algorithms, the implementation steps of particle swarm optimization are much more concise (the genetic algorithm includes three processes of inheritance, hybridization and

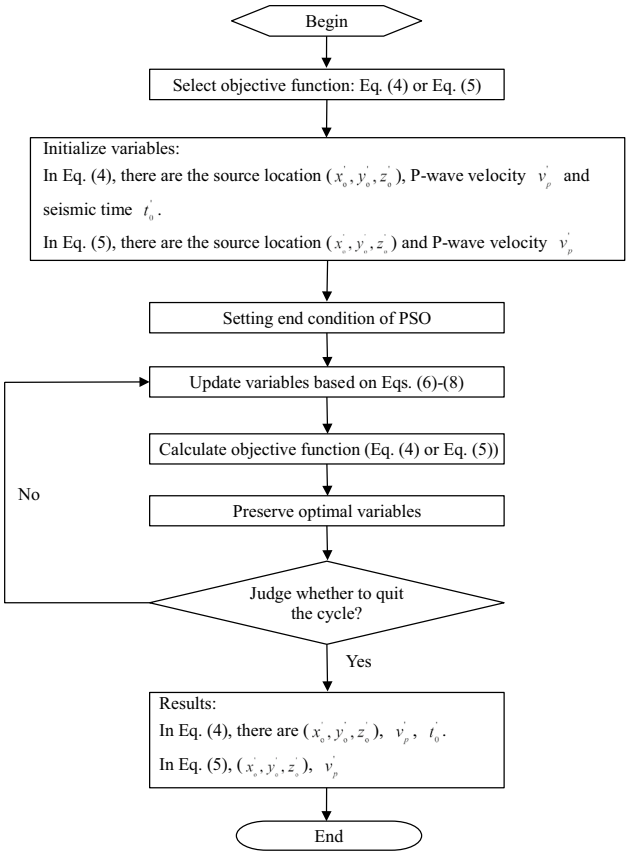

Fig. 5 The flow chart of the improved method

Table 2 Geophone coordinates and observations [10]

Geophone	*X* (m)	*Y* (m)	*Z* (m)	Observed time (ms)
A	67,354.79	52,037.4	538.7161	36.49
B	67,315.86	52,011.14	533.1324	42.50
C	67,276.13	51,998.22	548.0021	52.06
D	67,342.23	52,070.47	498.8039	31.79
E	67,296.19	52,044.93	497.5552	40.79
F	67,326.33	52,170.57	429.3200	34.10
G	67,236.59	52,121.75	430.1000	49.74

mutation). Particle swarm optimization is the most concise optimization one until now.

5 Engineering example

5.1 Case 1

Data for the observation of each event by the geophones are presented in Table 2 [10]. The source location of the event is located by the method proposed in this paper. The proposed method (method 1, Eq. (4) is used to describe the objective function) is compared with a localization method based on the arrival time (method 2). Because the proposed method mainly focuses on an improved objective function, specific search algorithms such as GA and PSO are not compared. Therefore, based on the two methods, PSO is used for the search process, which is computed by MATLAB.

The same two-parameter set (population number of 50, evolution algebra of 2000) was applied in each method, and the results are presented in Table 3. The source location given by method 1 is (67,429.98 m, 52,080.40 m, 430.26 m), and that given by method 2 is (67,430.70 m, 52126.32 m, 478.74 m). The actual source location is (67,464.76 m, 52,109.28 m, 441.29 m).

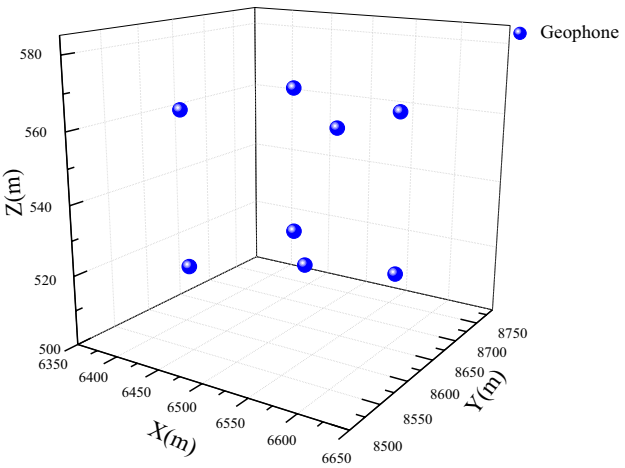

Fig. 6 Positional arrangement of the geophones for case 2

Table 3 Results calculated by the two methods

Case	Method 1			Method 2			Actual source location		
	x_o (m)	y_o (m)	z_o (m)	x_o (m)	y_o (m)	z_o (m)	x_o (m)	y_o (m)	z_o (m)
1	67,429.98	52,080.40	430.26	67,430.70	52,126.32	478.74	67,464.76	52,109.28	441.29
2	6515.50	8674.40	534.30	6494.90	8633.30	564.40	6597.50	8704.10	534.80

Table 4 Error analysis of the two methods

Case	Method 1				Method 2			
	X (m)	Y (m)	Z (m)	d_1 (m)	X (m)	Y (m)	Z (m)	d_2 (m)
1	34.78	28.88	11.03	46.53347	34.06	− 17.04	− 37.45	53.41299
2	82	29.7	0.5	87.21433	102.6	70.8	− 29.6	128.1232

An improved positioning accuracy is defined as:

$$p = \frac{d_2 - d_1}{d_2} \times 100\%, \tag{9}$$

where d_1 is the positioning error (the Euclidean distance between the actual source and method 1) of method 1 and d_2 is the positioning error of method 2 (the Euclidean distance between the actual source and method 2). Both methods can show relatively accurate source locations. The calculated results indicate that the accuracy of method 1 is about 14% better than that of method 2.

5.2 Case 2

The geophone layout scheme [3] shown in Fig. 6 consists of eight geophones. The two methods used in case 2 were used to locate the source of the event.

The parameters for each method were as described above (population number of 50, evolutionary algebra of 1000). The results are presented in Table 3. The localization result given by method 1 is (6515.50 m, 8674.40 m, 534.30 m), whereas that given by method 2 is (6494.90 m, 8633.30 m, 564.40 m). The actual source location in this event is (6597.50 m, 8704.10 m, 534.80 m). The localization results of method 1 are more than 32% better than those of method 2 in Table 4.

6 Conclusions

1. The actual wave velocity is anisotropic. Using the time of arrival or the time difference method, the wave velocity is anisotropic. Therefore, it is difficult to ignore the effect of the velocity error on positioning.
2. A new inverse objective function has been proposed by combining the advantages of the L2 norm function and the variance function. The effectiveness of the proposed method was verified by two case studies. This objective function can assess the accuracy and ensure the stability of the positioning results. Deviations in the accuracy at different geophone positions can be prevented.

Acknowledgements We wish to thank the National Natural Science Foundation of China (No. 41672282), State Key Laboratory of Geohazard Prevention and Geoenvironment Prevention Independent Research Project (No. SKLGP2017Z003), the Opening Fund of the State Key Laboratory of Geohazard Prevention and Geoenvironment Protection (Chengdu University of Technology) (No. SKLGP2017K008), and the first author thanks the Innovative Team of Chengdu University of Technology.

Compliance with ethical standards

Conflict of interest The authors declare that they have no conflict of interest.

References

1. Behrouz G, Danial JA, Mohsen H, Masoud M (2016) Prediction of seismic slope stability through combination of particle swarm optimization and neural network. Eng Comput 32:85–97
2. Cheng MY, Hoang ND (2015) Typhoon-induced slope collapse assessment using a novel bee colony optimized support vector classifier. Nat Hazards 78:1961–1978
3. Chen BR, Feng XT, Li SL, Yuan JP, Xu SC (2009) Microseismic sources location with hierarchical strategy based on particle swarm optimization. Chin J Rock Mech Eng 28(4):740–749 **(in Chinese)**
4. Dai F, Li B, Xu NW, Fan YL, Zhang CQ (2016) Deformation forecasting and stability analysis of large-scale underground powerhouse caverns from microseismic monitoring. Int J Rock Mech Min Sci 86:269–281
5. Dong LJ, Li XB (2013) A microseismic/acoustic emission source location method using arrival times of PS waves for unknown velocity system. Int J Distrib Sens Netw. https://doi.org/10.1155/2013/307489
6. Douglas A (1967) Joint epicenter determination. Nature 215:45–48
7. Ewan JS, Milton OK, Lindsay ML (2003) Source parameters of acoustic emission events and scaling with mining-induced seismicity. J Geophys Res 108(B9):2418
8. Felix G, Stefan E (2016) Installation of a microseismic monitoring system in the Mittersill scheelite mine. Geomech Tunn 9(5):515–523
9. Feng GL, Feng XT, Chen BR, Xiao YX, Jiang Q (2015) Sectional velocity model for microseismic source location in tunnels. Tunn Undergr Space Technol 45:73–83
10. Gao YT, Wu QL, Wu SC, Ji MW, Yang K, Liu C (2015) Source parameters inversion based on minimum error principle. J Cent South Univ (Sci Technol) 46(8):3054–3060 **(in Chinese)**
11. Geiger L (1912) Probability method for the determination of earthquake epicentres from the time of arrival only. Bull St Louis Univ 8:60–71
12. Ge MC (2012) Source location error analysis and optimization methods. J Rock Mech Geotech Eng 4(1):1–10
13. He J, Dou LM (2012) Gradient principle of horizontal stress inducing rock burst in coal mine. J Cent South Univ 19:2926–2932
14. Jane MA, Peter KK, Brad PS (1998) Use of microseismic source parameters for rockburst hazard. Pure Appl Geophys 153:41–65
15. Li A, Dai F, Xu NW, Gu GK, Hu ZH (2019) Analysis of a complex flexural toppling failure of large underground caverns in layered

rock masses. Rock Mech Rock Eng. https://doi.org/10.1007/s00603-019-01760-5
16. Li B, Li T, Xu NW, Dai F, Chen WF, Tan YS (2018) Stability assessment of the left bank slope of the Baihetan Hydropower Station, Southwest China. Int J Rock Mech Min Sci 104:34–44
17. Li J, Wu SC, Gao YT, Li LJ, Zhou Y (2015) An improved multi-directional velocity model for micro-seismic monitoring in rock engineering. J Cent South Univ 22:2348–2358
18. Li LL, He C, Tan YY (2017) Study of recording system and objective function for microseismic source location. Acta Scientiarum Naturalium Universitatis Pekinensis 53(2):329–343 **(in Chinese)**
19. Li N, Ge MC, Wang EY (2014) Two types of multiple solutions for microseismic source location based on arrival-time-difference approach. Nat Hazards 73:829–847
20. Li N, Wang EY, Ge MC, Sun ZY, Sun ZY (2014) A nonlinear microseismic source location method based on simplex method and its residual analysis. Arab J Geosci 7:4477–4486
21. Li XB, Dong LJ (2011) Comparison of two methods in acoustic emission source location using four sensors without measuring sonic speed. Sens Lett 9(5):1501–1505
22. Li Y, Yang TH, Liu HL, Wang H, Hou XG, Zhang PH, Wang PT (2016) Real-time microseismic monitoring and its characteristic analysis in working face with high-intensity mining. J Appl Geophys 132:152–163
23. Ma CC, Li TB, Xing HL, Zhang H, Wang MJ, Liu TY, Chen GQ, Chen ZQ (2016) Brittle rock modeling approach and its validation using excavation-induced micro-seismicity. Rock Mech Rock Eng 49:3175–3188
24. Salvoni M, Dight PM (2016) Rock damage assessment in a large unstable slope from microseismic monitoring-MMG Century mine (Queensland, Australia) case study. Eng Geol 210:45–56
25. Spence W (1980) Relative epicenter determination using P-wave arrival-time differences. Bull Seismol Soc Am 70(1):171–183
26. Van AG, Butler AG (1993) Applications of quantitative seismology in South African gold mines. In: Proceedings of 3rd international symposium rockbursts and seismicity in mines, pp 41–48
27. Wu LZ, Zhou Y, Sun P, Shi JS, Liu GG, Bai LY (2017) Laboratory characterization of rainfall-induced loess slope failure. CATENA 150:1–8
28. Wu LZ, Deng H, Huang RQ, Zhang LM, Guo XG, Zhou Y (2019) Evolution of lakes created by landslide dams and the role of dam erosion: a case study of the Jiajun landslide on the Dadu River, China. Quat Int 503A:41–50
29. Wu LZ, Shao GQ, Huang RQ, He Q (2018) Overhanging Rock: Theoretical, Physical and Numerical Modeling. Rock Mech Rock Eng 51(11):3585–3597
30. Wu LZ, Li SH, Zhang M, Zhang LM (2019) A new method for classifying rock mass quality based on MCS and TOPSIS. Environl Earth Sci 78(6):199
31. Xu NW, Li TB, Dai F, Zhang R, Tang CA, Tang LX (2016) Microseismic monitoring of strainburst activities in deep tunnels at the Jinping II hydropower station, China. Rock Mech Rock Eng 49:981–1000
32. Zhang M, Wu LZ, Zhang JC, Li LP (2019) The 2009 Jiweishan rock avalanche, Wulong, China: deposit characteristics and implications for its fragmentation. Landslides 16(5):893–906